Table 1: Summary of datasets used in this study. The meteorological forcing fields include precipitation (precip), downward long-wave radiation (LW), downward shortwave radiation (SW), air temperature (Ta), specific humidity (Q), surface air pressure (P), zonal (U), and meridional (V) wind speed.

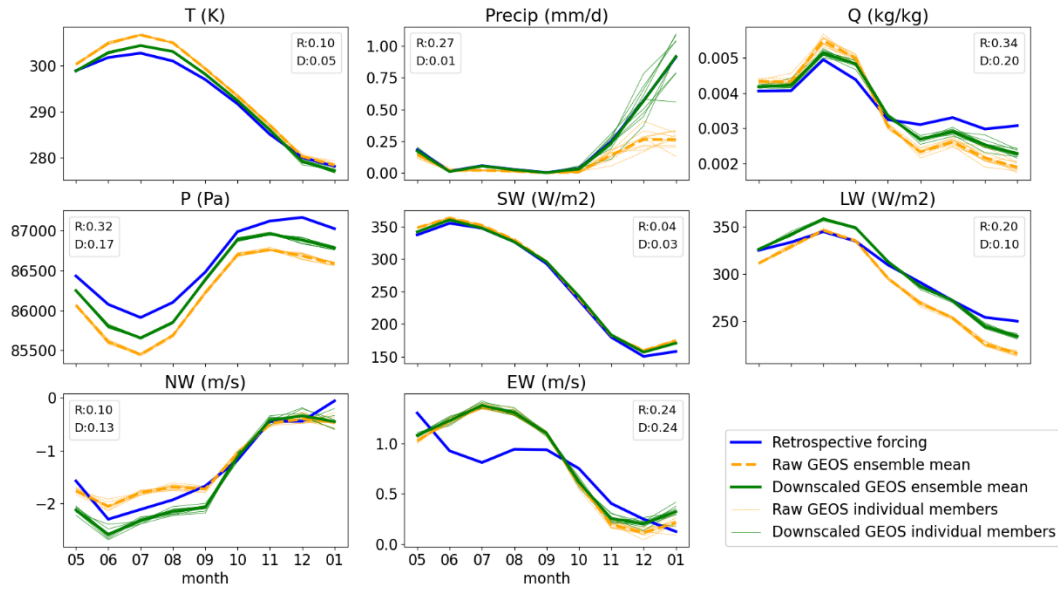| Data	Period of Record	Spatial resolution	Temporal resolution	Variable used	Reference
CHIRPS	1981-present	0.05°	1 day	Precip	Funk et al., 2015
GDAS	2000-present	1° × 1° gradually improved to 0.125° × 0.125°	6 hours	LW, SW, Ta, Q, P, U, V	National Climatic Data Center, 2020
GEOS-S2S-V1	1981-2018 Jan	1°×1.25°	1 day	Precip, LW, SW, Ta, Q, P, U, V	Borovikov et al., 2017
GEOS-S2S-V2	1981-present	0.5°×0.5°	1 day	Precip, LW, SW, Ta, Q, P, U, V	Molod et al., 2020
ESA-CCI SM	1978 Nov - 2019 Dec	0.25°×0.25°	1 day	Surface soil moisture	Gruber et al., 2019

Figure S1: Comparison of Air temperature (T), precipitation (Precip), specific humidity (Q), surface pressure (P), solar radiation (SW), longwave radiation (LW), north-south wind speed (NW), east-west wind speed (EW) among Retrospective, raw GEOS-S2S-V1 and downscaled GEOS-S2S-V1 meteorological forcing in the Helmand basin. The root mean squared error normalized by the range of the retrospective meteorological forcing (NRMSE) is shown as the values in each subplot. R denotes the NRMSE between raw GEOS-S2S-V1 and retrospective forcing and D denotes the NRMSE between downscaled GEOS-S2S-V1 and retrospective forcing.
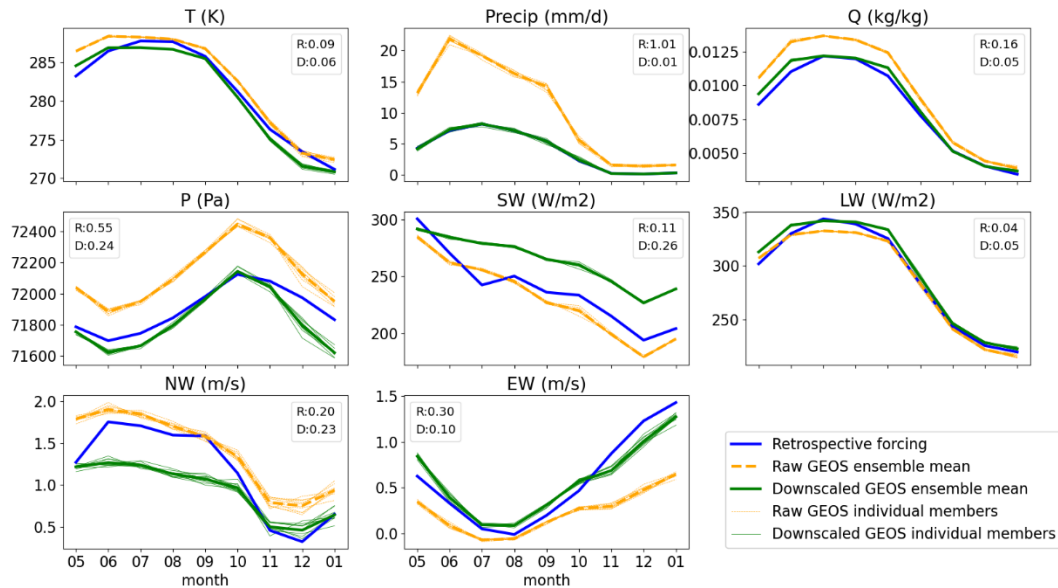

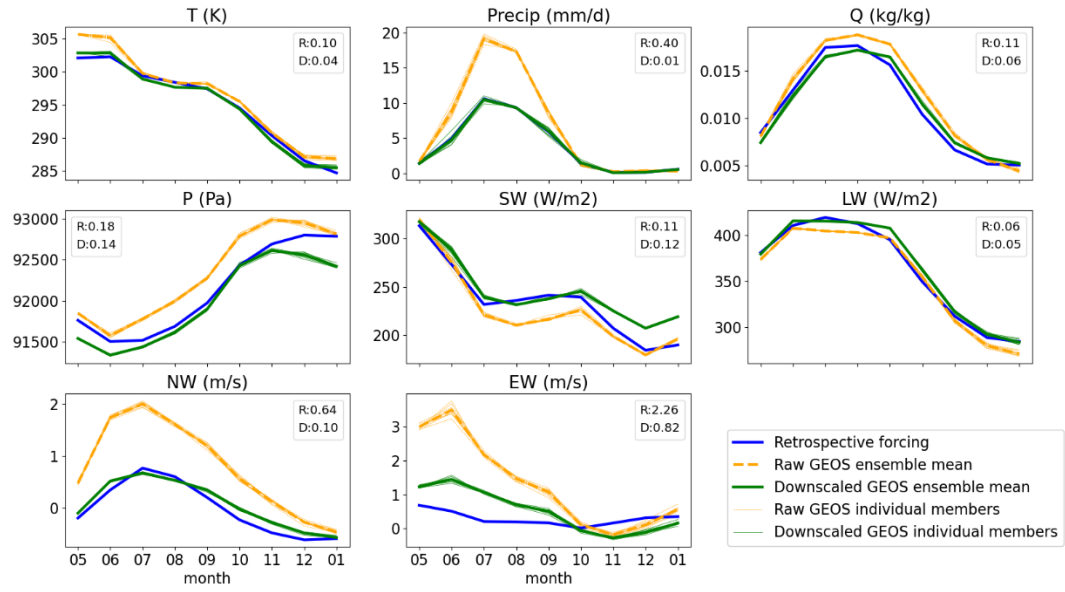**Figure S2: The same as Fig. S1 but in the Brahmaputra basin.**

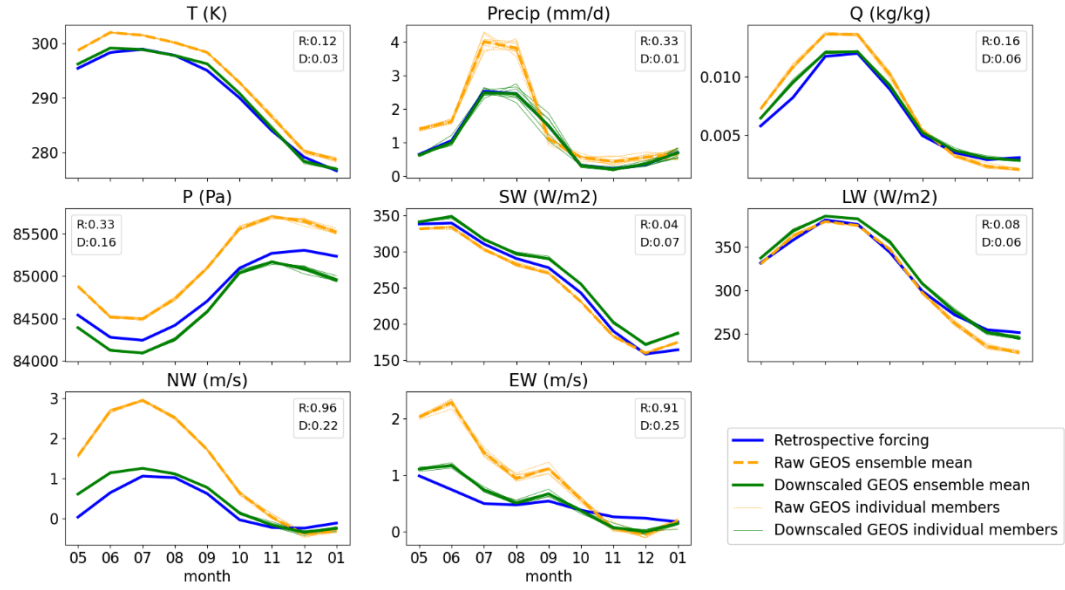**Figure S3: The same as Fig. S1 but in the Ganges basin**

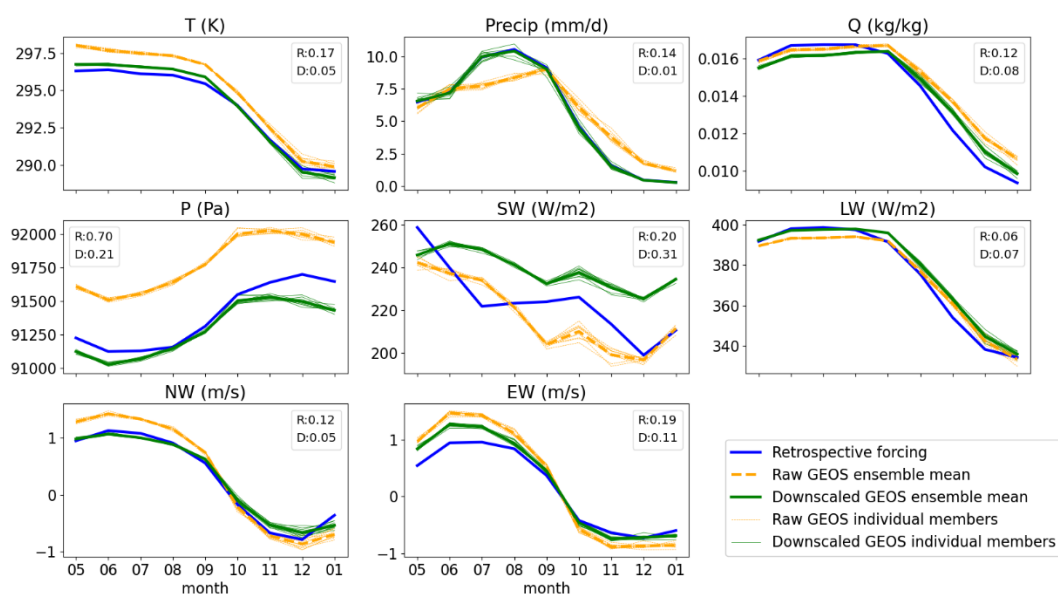**Figure S4: The same as Fig. S1 but in the Indus basin**

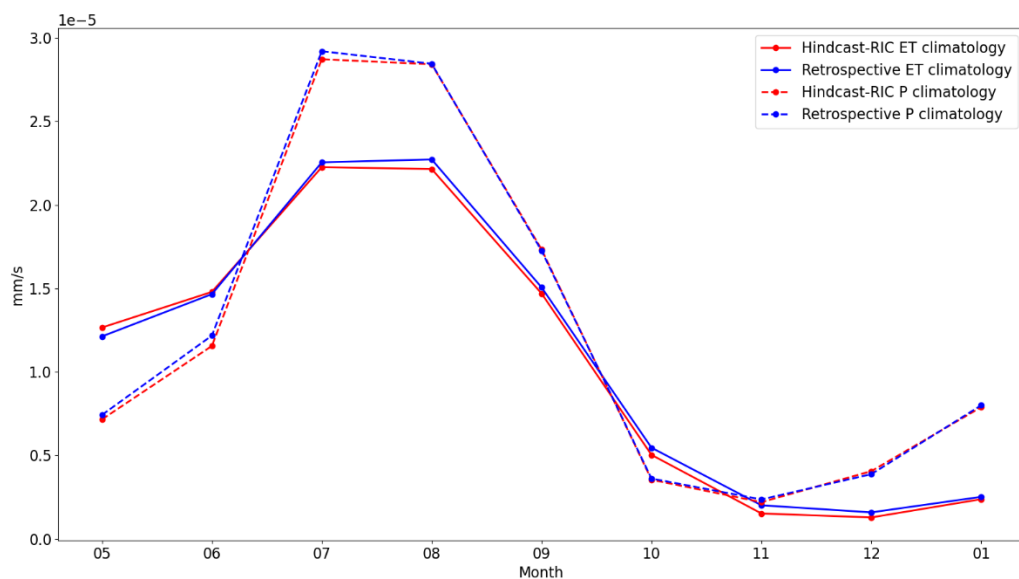**Figure S5: The same as Fig. S1 but in the Mekong basin**

Figure S6. The climatological monthly precipitation and evapotranspiration (ET) in the Indus basin from retrospective and hindcast-RIC simulations.
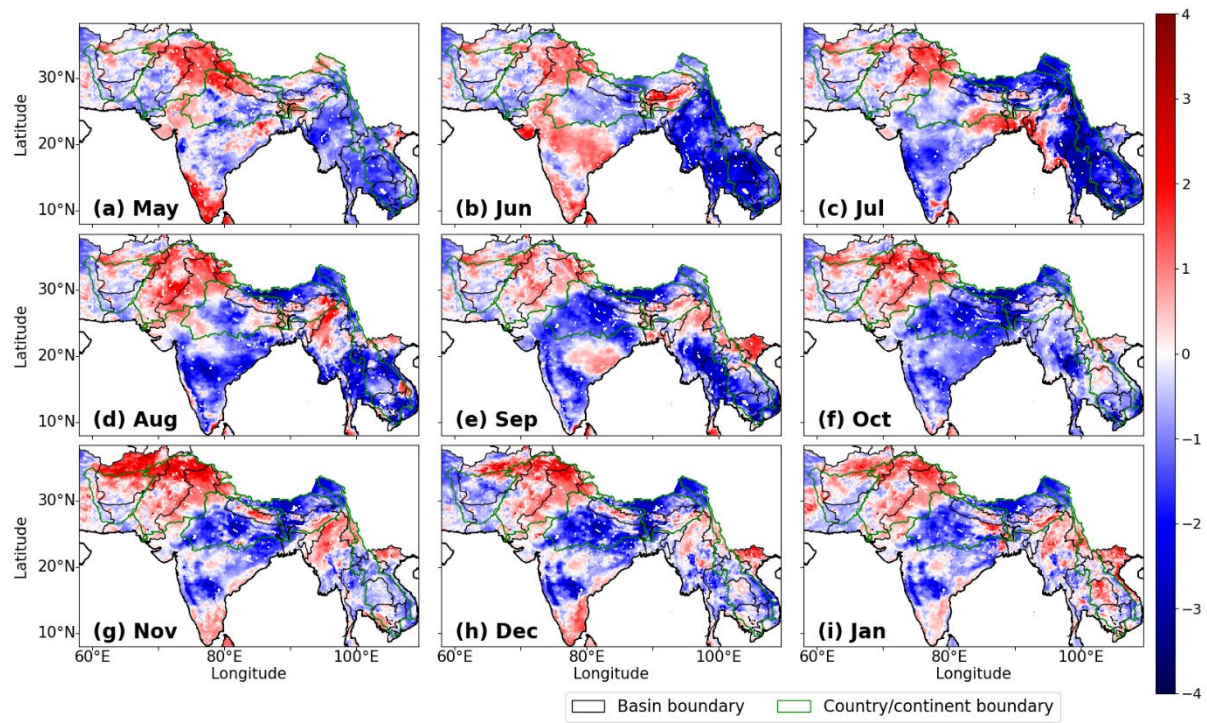
Figure S11. The spatial distribution of monthly RZSM standardized anomaly for 2015 South and Southeast Asia drought calculated from the retrospective simulation
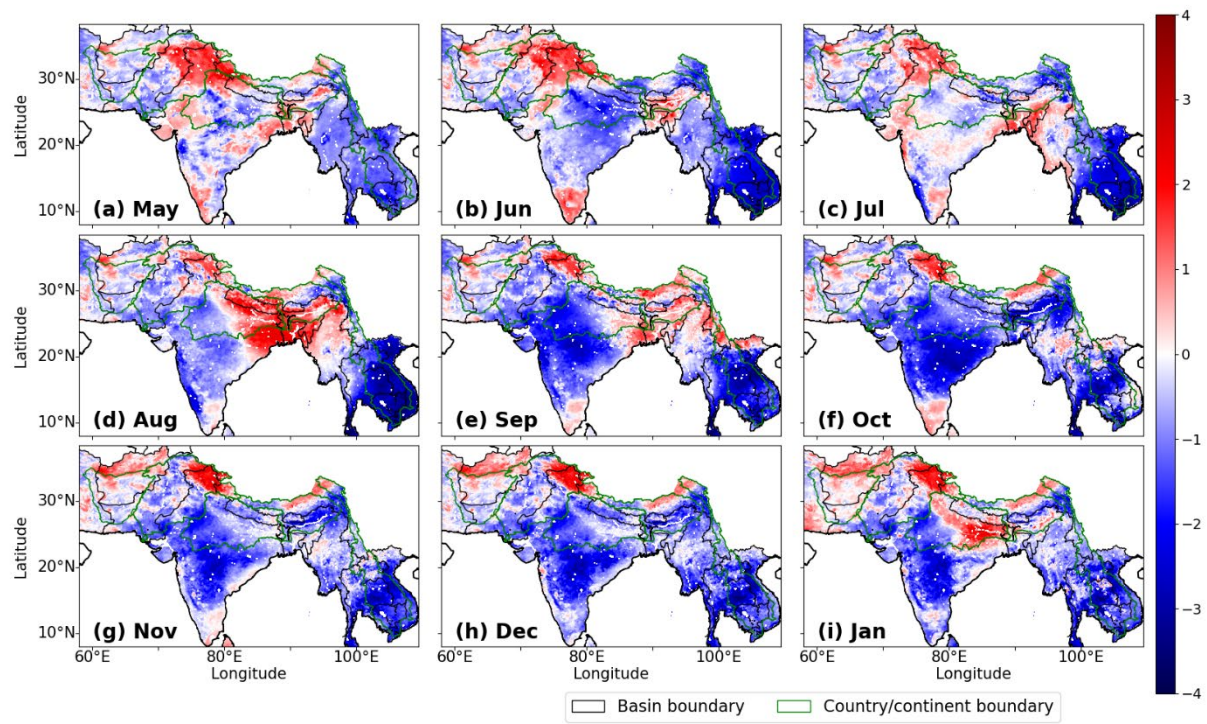
Figure S12. The same as Fig. S12 but calculated from ensemble mean of the hindcast-RIC simulation